

Measuring the quantum efficiency of single radiating dipoles using a scanning mirror

B. C. Buchler,¹ T. Kalkbrenner,^{1,*} C. Hettich,^{1,†} and V. Sandoghdar^{1,‡}

¹*Laboratory of Physical Chemistry, Swiss Federal Institute of Technology (ETH), 8093 Zurich, Switzerland.*

(Dated: November 13, 2018)

Using scanning probe techniques, we show the controlled manipulation of the radiation from single dipoles. In one experiment we study the modification of the fluorescence lifetime of a single molecular dipole in front of a movable silver mirror. A second experiment demonstrates the changing plasmon spectrum of a gold nanoparticle in front of a dielectric mirror. Comparison of our data with theoretical models allows determination of the quantum efficiency of each radiating dipole.

It is a well established matter that the radiation of an oscillating electric dipole can be manipulated if it is placed in front of a planar interface [1]. Experiments investigating this system date back to Drexhage [2] who looked at the influence of a metallic mirror on the fluorescence lifetime of ensembles of Eu^{3+} ions. By preparing a large number of samples, each with a different spacing between the mirror and the emitter layer, two major effects were observed. Firstly, it was shown that the decay rate (Γ) oscillates at large distances due to the retarded interaction of the dipoles with their own reflected fields. Secondly, it was shown that Γ is strongly modified very close to the mirror due to the energy transfer to the metal [1, 2]. Since that time, numerous works have investigated the modification of spontaneous emission from ensembles in thin dielectric layers [1]. Various key parameters such as the dipole's orientation, its distance to the interface and its quantum efficiency are, however, averaged in ensemble measurements.

Due to challenges such as detection sensitivity, photostability and position control, experiments with single emitters have been scarce. Some researchers have nevertheless shown effects of the local dielectric environment by adding an index matching fluid to eliminate an interface [3, 4] or by introducing the subwavelength boundary of a sharp tip [5, 6]. In this work we study the fluorescence lifetime and intensity of a single molecule at a well-defined orientation and position, while moving an external silver mirror in its vicinity. We also examine the plasmon spectrum of a well-characterized single gold nanoparticle at various locations in front of a dielectric mirror. These experiments allow us to demonstrate, for the first time, both the far-field modulation and the near-field modification of the total decay rate (Γ) for individual dipoles. Since the far-field modulations are only due to changes in the radiative decay rate (Γ_r) we can determine the quantum efficiency $\eta = \Gamma_r/\Gamma$ of each dipole.

A theoretical description of dipole decay in multi-layer structures was first developed by Chance et al. [7] and has been expanded by many authors to cover numerous

situations. In particular, Sullivan and Hall [8] present an elegant plane wave solution that can easily be adapted to our system. For a single dipole at angle θ with respect to the normal of the dielectric layers we find [9]:

$$\Gamma = \Gamma_0[1 - \eta_0 + \eta_0(V \cos^2 \theta + H \sin^2 \theta)] \quad (1)$$

where η_0 and Γ_0 are the quantum efficiency and decay rate, respectively, in bulk dielectric. The functions V and H are, respectively, the normalised decay rates of dipoles perpendicular and parallel to the layers. These functions depend on the position of the dipole, as well as the thickness and refractive indices of the various layers.

The essential feature of our experimental system was the combination of an inverted microscope and a shear-force controlled scanning probe stage [10]. A schematic of the setup used for the single molecule measurements is shown in Fig. 1A. Samples of highly photostable terrylene molecules embedded in a thin para-terphenyl (pT) matrix were prepared following the method described in [11]. The thickness (t) of the pT layer in this work was $35 \pm 5 \text{ nm}$ as measured using shear-force microscopy. The sample was illuminated through an oil immersion objective (NA=1.4) by 13 ps pulses of p-polarized 532 nm light at a repetition rate of 5 MHz. The laser light was focused in the back focal plane of the objective to give a near-collimated beam at the pT layer. An offset of the beam at the back focal plane resulted in an incidence angle ϕ and total internal reflection at the pT-air interface. The fluorescence of the terrylene ($\lambda \sim 580 \text{ nm}$) was collected confocally through the objective and sent to an avalanche photodiode (APD) for lifetime measurements or to a CCD for imaging. Above the pT layer we mounted a micro-mirror in the shear-force stage. The mirror was made by melting the end of a tapered optical fibre to give a ball of diameter $40 \mu\text{m}$, then coating this ball with 200 nm of silver. Using the scanning stage, the mirror was lowered onto the pT layer, bringing it into shear-force contact at a height z_0 . This point of closest separation was in the range 5 to 20 nm. The calibrated piezo used in the z-axis of the system thus gave an accurate measurement of the mirror-pT distance (z) relative to the zero defined by z_0 . The lateral position of the mirror against a molecule was optimized by maximizing the quenching of the fluorescence with the mirror at z_0 .

Figure 1B shows the image obtained when the fluorescence from a single molecule, measured without the

*Present address:FOM-Institute for Atomic and Molecular Physics (AMOLF), 1098 SJ Amsterdam, The Netherlands

†Present address:Niels Bohr Institute, 2100 Copenhagen, Denmark

‡Electronic address: vahid.sandoghdar@ethz.ch

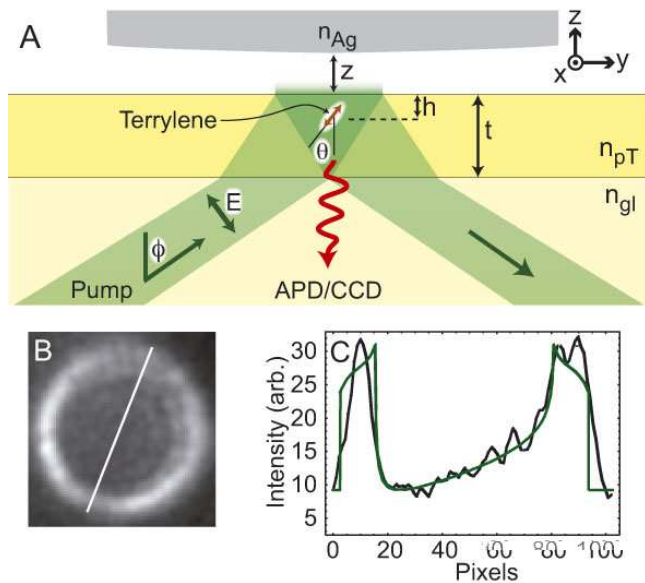


FIG. 1: A: Terrylene molecules embedded in para-terphenyl (pT) were illuminated by p-polarized light that undergoes total internal reflection at the pT-air interface. A silver micro-mirror was positioned in front of the sample with a three-dimensional piezo stage (not shown). Fluorescence light is collected and sent to an APD or CCD camera. Parameters used in the modelling are defined in this diagram. B: The intensity distribution at the back focal plane for a single molecule (with no mirror). C: A cross section indicated in B. A fit to this data shows a dipole angle θ of 16 ± 5 degrees.

mirror, is collected by the objective and sent directly to the CCD with no further imaging optics. The highly directional (doughnut like) emission stems from the fact that the terrylene dipole is oriented nearly perpendicular to the substrate plane [11]. As has been shown very recently [12], by analyzing this image we can determine the tilt angle θ of the dipole. From the cross section in Fig. 1C we find $\theta = 16 \pm 5$ degrees.

Fluorescence lifetime ($\tau = 1/\Gamma$) was measured via time-correlated single photon counting. Photon arrival times were histogrammed and an exponential decay curve was fitted to find the excited state lifetime. To achieve the required accuracy, 1 to 2 s of data were required per measurement. In bulk pT the lifetime of terrylene is $\tau_0 = 1/\Gamma_0 = 4.1 \pm 0.1$ ns [13]. In our system (without the micro-mirror) lifetimes were in the range 15 to 25 ns. Increased lifetime is expected for molecules embedded in thin dielectric films [14]. This effect can be described using Eq. 1 and, due to the dependencies of V and H , is highly sensitive to the dipole orientation and depth of the molecule in the film. A particular virtue of single emitter studies is their ability to deal with such inhomogeneities.

We now turn to the lifetime measurements of single molecules as a function of the mirror position z . During the course of the experiment, data was collected from around 15 different molecules. Shown in Fig. 2 are two of these measurements. The lifetime was monitored as

the mirror moved towards and away from the molecule, thereby verifying the mechanical stability of the system and lack of any drifts. We note that more than 5×10^7 photons were detected per molecule, emphasizing the advantage of a sample with very high photostability [11].

The data in Fig. 2 clearly shows the near-field shortening of the lifetime due to quenching by the metal as well as far-field oscillations that can be understood as being due to the retarded interaction of the dipole with its mirror image [1, 2]. The solid curves in the figure show fits to the data made using Eq. 1. The refractive indices n_{gl} and n_{Ag} of glass and silver at 580 nm are taken to be 1.52 and $0.26 + 4i$, respectively. Paraterphenyl is bi-axial with refractive indices $n_z = 2.0$, $n_y = 1.69$ and $n_x = 1.59$ [11, 15]. In the calculations we take the out-of-plane polarizations to have an index of $(n_x + n_y)/2 = 1.64$. For polarizations parallel to the plane of incidence we assume an index of 1.85 [16]. Using these assumptions, the unknown parameters η_0 , h and z_0 can be approximated by fitting the model to the data. For molecule A we find $0 < h < 13$ nm, $0.9 < \eta_0 < 1$ and $z_0 = 12 \pm 2$ nm whereas for B, $12 < h < 32$ nm, $0.9 < \eta_0 < 1$ and $z_0 = 11 \pm 5$ nm. These values are consistent with what we know about our system. Molecules with longer lifetimes are expected to have smaller depth (h) and the offset (z_0) agrees well with the typical shear-force interaction range of $z_0 < 20$ nm. The estimates of η_0 and h are limited by the uncertainty in the dipole orientation θ , a parameter that is integrated out in the theoretical treatments of ensembles, but plays a central role in single emitter studies [4].

The fluorescence intensity is also measured using the APD. For molecule B of Fig. 2 this is shown in Fig. 3I along with the lifetime data (curve II). For large z , there is a clear correlation between the intensity and lifetime. The strong intensity modulation is due to our detection optics only seeing a part of the emission pattern while the

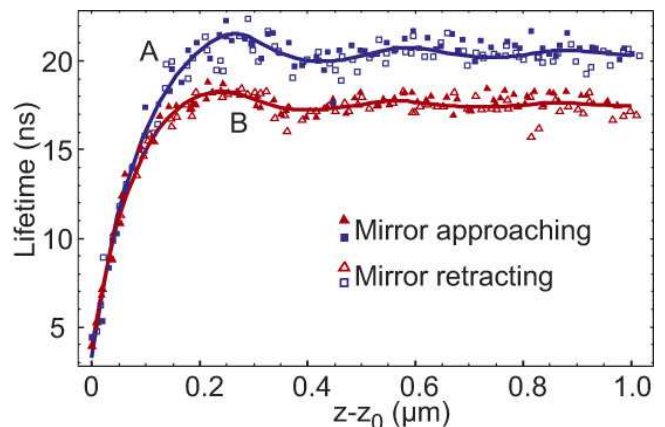


FIG. 2: Lifetime as a function of mirror position (z) for 2 molecules A (squares) and B (triangles). The solid curves display theoretical fits assuming $\eta_0 = 0.98$, $h = 3$ nm and $z_0 = 12$ nm for A, $\eta_0 = 1$, $h = 22$ nm and $z_0 = 11$ nm for B and $\theta = 16^\circ$ in both cases.

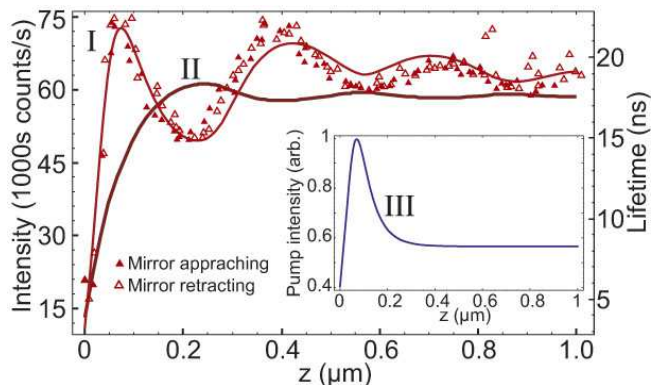


FIG. 3: I (left-hand axis): Symbols show measured intensity of molecule B in Fig. 2. The curve is the theoretical fit to the data with fitted parameters of $\phi = 53 \pm 1$, $NA = 1.00 \pm 0.01$ and other variables as in Fig. 2. II (right-hand axis): The curve B of Fig. 2. III: The pump intensity at the position of the molecule with $\phi = 53^\circ$.

angular distribution of the fluorescence is changing with the mirror position. The modification of emission patterns in the presence of planar boundaries was originally described by Drexhage [2] and more recently exploited in the design of semiconductor cavities [17].

The fluorescence intensity can be modelled by finding the emission pattern and then integrating over the numerical aperture of the collection optics [18, 19]. As shown by Fig. 3III, we must also consider the change in pump intensity experienced by the molecule when the mirror enters the evanescent field above the pT surface. As our measurements were made well below the pump saturation level, we just multiply the integrated emission pattern by the pump intensity. The solid curve in Fig. 3I shows the theoretical fit to the intensity data, displaying reasonable agreement. We note that although the numerical aperture of our objective was 1.4, the intensity modulation is best reproduced by $NA=1$. Numerous factors, such as misalignment of the detection optics or the birefringence of the pT film, could lead to a reduction of the effective numerical aperture. We believe that the main cause of the discrepancy is that the integration of the emission pattern over the numerical aperture assumes the entire dipole-mirror system is at the focus of the objective. This is not actually the case for $z > 500$ nm, equivalent to a Rayleigh range of the microscope objective. In this regime our high NA confocal detection system begins to lose some of the photons that are first emitted upward and then reflected by the mirror.

We will now consider the second experimental system, namely a gold nanoparticle in front of a glass substrate. A gold particle can support plasmon resonances that stem from the collective oscillation of electrons in the metal [20]. The spectrum of the plasmon resonance depends on the size and shape of the particle, as well as the complex dielectric constants of the particle and surrounding medium. In general, the scattering and absorption

properties of a nanoparticle can be described by a multipole expansion. For gold particles smaller than about 100 nm, it suffices to consider only a dipolar oscillation if one accounts for the effect of radiation damping [21]. In an ellipsoidal particle, up to 3 dipolar oscillations can be excited yielding independent plasmon resonances at 3 different frequencies [20]. In a recent publication we have demonstrated a tomographic approach to identify these resonances and find the orientation of the particle axes in the laboratory frame [22]. Furthermore, in [23] we presented a recipe for attaching a single nanoparticle to the extremity of a sharp optical fiber. Here we exploit these techniques to first characterize an ellipsoidal nanoparticle (nominal diameter of 80 nm) attached to a fiber tip and then monitor the width of one of its plasmon resonances as we move the particle relative to a glass substrate.

Details of the setup and the spectroscopy procedure are given in [22]. In short, the system was illuminated at grazing incidence with white light from a xenon lamp (see Fig. 4III). The scattered light was collected by a microscope objective ($NA=0.85$) through the glass substrate and sent to a spectrometer. By performing a tomographic measurement as described in [22], we determined the long axis of the particle to be oriented at $\theta = 10^\circ \pm 2^\circ$. We then rotated the tip about its axis as well as the polarization of the illumination to excite only the long axis plasmon. Figure 4II shows the measured plasmon spectrum and a fit obtained using the dipole term of Mie theory with a radiation damping correction [22].

A scanning piezo stage was used to control the distance (z) between the gold particle and a microscope coverglass ($n_{gl} = 1.52$). The point of closest approach (z_0) was found, as in the case of the single molecules, using a shear force signal. The plasmon decay time was found according to $\tau = 1/(2\pi\gamma)$ [24], where γ (in Hz) is the full-width at half-maximum of the resonance. A plot

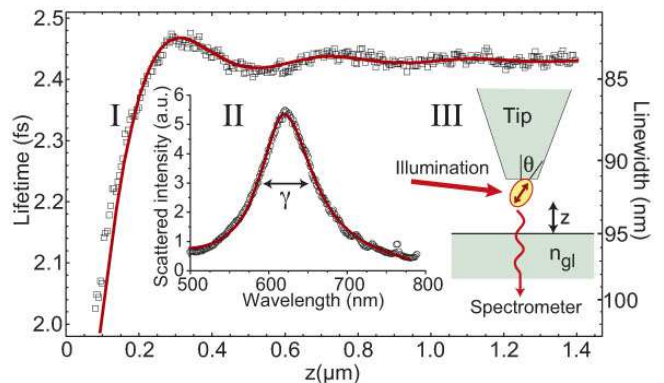


FIG. 4: I: The squares show the measured decay time and linewidth of the plasmon oscillations. The solid line shows a theoretical fit using Eq. 1. A stretch factor of 0.8 was fitted to the z axis as the piezo in this system was not calibrated. II: Circles show a plasmon spectrum recorded from the nanoparticle at the tip. The solid curve is a fit according to a modified Mie theory. III: A schematic of the setup.

of the plasmon lifetime (and linewidth on the right-hand axis) as a function of z is shown in Fig. 4I. This result qualitatively resembles that of the molecular dipole. In particular for large z we see slowly dying oscillations of the lifetime that eventually relax to a value of 2.43 fs. As shown by the solid curve in Fig. 4I, the data is well reproduced by a theoretical fit according to Eq. 1 [25]. Fitted parameters in this case were $z_0 = 9 \pm 6$ nm and $\eta_0 = 0.64 \pm 0.07$. There are two complications in this data that are unique to the gold plasmon measurements. Firstly, the agreement between theory and experiment deteriorates for $z < 200$ nm. We believe that this is because a gold particle close to the glass surface can be no longer treated as a point dipole. Data with $z < 250$ nm is therefore excluded from the fit. Secondly, the linewidth measurement is affected by interference between the plasmon scattering and stray excitation light [26] that causes a small but constant modulation of the linewidth at large z . This artifact, with peak-to-peak amplitude 0.007 fs and period equal to half the plasmon centre wavelength, has been subtracted from the data.

The so-called “quantum efficiency” for a classical antenna, such as a gold particle, can again be defined as $\eta = \frac{\Gamma_r}{\Gamma}$ whereby here Γ_r and Γ denote the scattering (radiation) and total plasmon relaxation rates, respectively [24, 27]. Equivalently, this quantity can be written as

$\eta = \frac{\sigma_s}{\sigma_s + \sigma_a}$ where σ_s and σ_a denote the scattering and absorption cross sections of the particle, respectively. Using the outcome of the tomographic measurements and the specified particle size, we calculated the values of σ_s and σ_a according to Mie theory and obtained $\eta_0 = 0.69 \pm 0.07$. Considering the substantial uncertainty in the parameters that enter into the Mie calculation, the agreement between the calculated quantum efficiency and that extracted from the experiment is very good.

In summary, we have demonstrated the *in situ* modification of the decay rate for a single quantum emitter as well as a classical nano-antenna. In both cases the manipulation of a movable external mirror at large distances modifies the dipole’s radiative decay rate but leaves its nonradiative dissipation channels unaffected. This enables us to extract the quantum efficiency of a single dipole, a quantity that is nontrivial to determine even for ensembles [28]. Our approach could be extended to various emitters of current interest, ranging from dye molecules and semiconductor nanoparticles to nanotubes. Such measurements would allow the investigation of fluctuations due to variations in the structure of the emitter or its local environment.

We thank A.F. Koenderink and S. Kühn for assistance and fruitful discussions. This work was supported by the Swiss National Science Foundation.

-
- [1] W. L. Barnes, *J. Mod. Opt.* **45**, 661 (1998).
 [2] K. H. Drexhage, *Progress in Optics* **12**, 165 (1974).
 [3] J. Macklin, J. Trautman, T. Harris, and L. Brus, *Science* **272**, 255 (1996).
 [4] X. Brokmann, L. Coolen, M. Dahan, and J. P. Hermier, *Phys. Rev. Lett.* **93**, 107403 (2004).
 [5] W. P. Ambrose, P. M. Goodwin, J. C. Martin, and R. A. Keller, *Science* **265**, 364 (1994).
 [6] W. Trabesinger, A. Kramer, M. Kreiter, B. Hecht, and U. Wild, *Appl. Phys. Lett.* **81**, 2118 (2002).
 [7] R. R. Chance, A. Prock, and R. Silbey, *Adv. Chem. Phys.* **37**, 1 (1978).
 [8] K. G. Sullivan and D. G. Hall, *J. Opt. Soc. Am. B* **14**, 1149 (1997).
 [9] L. Novotny, *J. Opt. Soc. Am. A* **14**, 91 (1997).
 [10] K. Karrai and I. Tiemann, *Phys. Rev. B* **62**, 13174 (2000).
 [11] R. J. Pfab, J. Zimmermann, C. Hettich, I. Gerhardt, A. Renn, and V. Sandoghdar, *Chem. Phys. Lett.* **387**, 490 (2004).
 [12] M. A. Lieb, J. M. Zavislan, and L. Novotny, *J. Opt. Soc. Am. B* **21**, 1210 (2004).
 [13] G. S. Harms, T. Irngartinger, D. Reiss, A. Renn, and U. P. Wild, *Chem. Phys. Lett.* **313**, 533 (1999).
 [14] M. Kreiter, M. Prummer, B. Hecht, and U. P. Wild, *J. Chem. Phys.* **117**, 9430 (2002).
 [15] K. Sundararajan, *Z. Krist.* **93**, 238 (1936).
 [16] The choice of n is not so critical. The model fits our data well for $1.78 < n < 1.95$ and in all cases the value of η is greater than 0.90. The value of 1.85 was found by considering the fraction of power radiated parallel and perpendicular to the slow axis. Previous work has also successfully employed an average index [2, 29]. Biaxial layers could, in principle, be included in the model, however to our knowledge this has never been done.
 [17] H. Benisty, H. DeNeve, and C. Weisbuch, *IEEE J. Quant. Elect.* **34**, 1612 (1998).
 [18] H. Benisty, R. Stanley, and M. Mayer, *J. Opt. Soc. Am. A* **15**, 1192 (1998).
 [19] J. Enderlein, *Chem. Phys.* **247**, 1 (1999).
 [20] U. Kreibig and M. Vollmer, *Optical Properties of Metal Clusters* (Springer Berlin, 1995).
 [21] A. Wokaun, J. P. Gordon, and P. F. Liao, *Phys. Rev. Lett.* **48**, 957 (1982).
 [22] T. Kalkbrenner, U. Hakanson, and V. Sandoghdar, *Nano Lett.* **4**, 2309 (2004).
 [23] T. Kalkbrenner, M. Ramstein, J. Mlynek, and V. Sandoghdar, *J. Microsc.* **202**, 72 (2001).
 [24] C. Sönnichsen, T. Franzl, T. Wilk, G. von Plessen, J. Feldmann, O. Wilson, and P. Mulvaney, *Phys. Rev. Lett.* **88**, 077402 (2002).
 [25] The fiber tip has a negligible influence on the plasmon spectrum [22]. Moreover, we are only sensitive to *changes* of the plasmon due to the glass substrate while any influence of the tip is constant during the experiment.
 [26] T. Kalkbrenner *et al.*, In preparation.
 [27] E. J. Heilweil and R. M. Hochstrasser, *J. Chem. Phys.* **82**, 4762 (1985).
 [28] G. A. Crosby and J. N. Demas, *J. Phys. Chem.* **75**, 991 (1971).
 [29] R. M. Amos and W. L. Barnes, *Phys. Rev. B* **55**, 7249 (1997).